Ultrafast coherent dynamics of nonadiabatically coupled quasi-degenerate excited states in molecules: Population and vibrational coherence transfers

H. Mineo [a], M. Kanno [b], H. Kono [b], S.D. Chao [a], S.H. Lin [c,d], Y. Fujimura [b,d,*]

[a] *Institute of Applied Mechanics, National Taiwan University, Taipei 106, Taiwan*
[b] *Department of Chemistry, Graduate School of Science, Tohoku University, Sendai 980-8578, Japan*
[c] *Institute of Atomic and Molecular Science, Academia Sinica, Taipei 106, Taiwan*
[d] *Department of Applied Chemistry, Chiao-Tung University, Hsin-Chu 300, Taiwan*

ARTICLE INFO

ABSTRACT

Results of a theoretical study of ultrafast coherent dynamics of nonadiabatically coupled quasi-degenerate π-electronic excited states of molecules were presented. Analytical expressions for temporal behaviors of population and vibrational coherence were derived using a simplified model to clarify the quantum mechanical interferences between the two coherently excited electronic states, which appeared in the nuclear wavepacket simulations [M. Kanno, H. Kono, Y. Fujimura, S.H. Lin, Phys. Rev. Lett 104 (2010) 108302]. The photon-polarization direction of the linearly polarized laser, which controls the populations of the two quasi-degenerate electronic states, determines constructive or destructive interference. Features of the vibrational coherence transfer between the two coupled quasi-electronic states through nonadiabatic couplings are also presented. Information on both the transition frequency and nonadiabatic coupling matrix element between the two states can be obtained by analyzing signals of two kinds of quantum beats before and after transfer through nonadiabatic coupling.

© 2011 Elsevier B.V. All rights reserved.

1. Introduction

Considerable attention has been paid to ultrafast coherent dynamics of photophysical and photochemical processes in molecular systems. These processes include excitation transfer in a photosynthetic system [1], resonance excitation transfer in conjugated polymer chains [2], stilbene isomerization [3], and nonradiative transitions in pyrazine vapor [4]. In these systems, vibrational and/or electronic coherences are created by ultrashort laser pulses, as proved by observation of quantum beats by using time-resolved optical measurement methods such as ultrafast pump-probe and transient grating methods.

We have recently found by quantum dynamical simulations that transient unidirectional motions of π-electrons in an ansa (planar-chiral) aromatic ring molecule can be created along its ring by using ultrashort, linearly polarized UV laser pulses [5]. Unidirectional motions of π-electrons are created by coherent excitation of a pair of quasi-degenerate electronic excited states. Unidirectional rotational motions, clockwise or counterclockwise, can be controlled by changing the direction of the photon polarization of the pulses. Moreover the rotational direction of π-electrons can be controlled by changing the relative optical phase of a two-color

laser [6]. π-Electrons can be continuously rotated by applying a sequence of pump and dump pulses. We have also performed nuclear wavepacket simulations taking into account nonadiabatic couplings between the quasi-degenerate electronic states of the same molecular system, and found that the populations in the two electronic states strongly depend on the direction of linearly polarized photon polarization of the laser pulse applied [7]. We have also found that the frequency spectra, which were obtained by the Fourier transform of the autocorrelation spectra of the wavepackets, depend on the photon polarization direction of the laser pulse used [7]. The vibrational dynamics found is directly related to the rotational direction of π-electrons, clockwise or counterclockwise. Thus, the results of two types of the simulations mentioned above indicate that information on ultrafast π-electron dynamics can be obtained by observing coherent vibrational dynamics as well.

However, there remain issues to be clarified for a thorough understanding of coherent nuclear dynamics in nonadiabatically coupled quasi-degenerate π-electronic excited states. There was no explicit explanation of the photon polarization-dependent nuclear dynamics found by nuclear wavepacket simulations, although a qualitative explanation based on nuclear wavepacket interferences was given [7,8].

In this paper, we focus on the mechanism of the photon polarization dependent vibrational behaviors found by nuclear wavepacket simulations. We explicitly take into account the coherent

* Corresponding author.
E-mail address: fujimurayuichi@m.tohoku.ac.jp (Y. Fujimura).

dynamics in two optically allowed electronic excited states coupled with nonadiabatic couplings. For this purpose, we adopt a simplified one-dimensional model. We show that the photon polarization-dependent nuclear dynamical behaviors obtained by nuclear wavepacket simulations originate from quantum mechanical interferences between a coherently excited pair of quasi-degenerate excited states.

In addition to population changes through nonadiabatic couplings mentioned above, there is another class of coherent nuclear dynamics in molecular systems, vibrational coherence transfers. Bath-induced vibrational coherence transfers have already been treated theoretically [9,10]. In this paper, we treat vibrational coherence transfers through intramolecular nonadiabatic couplings as well. The concept of vibrational coherence in an electronic excited state and its transfer to a lower electronic state is essential to analyze nuclear wavepacket dynamics between two electronic states coupled by nonadiabatic interactions. Recently, Suzuki et al. [4] have reported quantum beats in time-resolved photoelectron imaging of ultrafast nonradiative transitions from an optically active $\pi\pi^*$ state of pyrazine by 20-fs laser pulses. The quantum beats reported originate from vibrational coherence transfer through nonadiabatic couplings. In general, quantum beats have different structures before and after the transfer through nonadiabatic coupling. We clarify features of vibrational coherence transfer and derive an expression for the amplitude and that for the frequency of beat signals of vibrational coherence.

In the next section, we present an analytical expression for photon polarization-dependent nonadiabatic coupling effects of coherently excited quasi-degenerate electronic states in a simplified model. Here, optical excitation processes were omitted except for the case in which comparison was made with results obtained by nuclear wavepacket simulations [7]. The wavepacket simulations of nonadiabatic dynamics in a model chiral aromatic molecule irradiated by a linearly polarized laser pulse were performed to clarify the effects of π-electron rotation on molecular vibration and vice versa [7]. In Section 3, we discuss the results of analysis of vibronic coherence effects dependent on photon-polarization. Vibrational coherence transfer induced by nonadiabatic couplings is also discussed.

2. Theoretical approach

Consider a nonadiabatic transition in a simplified potential model shown in Fig. 1a to explain the temporal behaviors found in the quantum dynamical simulations of 2,5-dicholoropyrazine
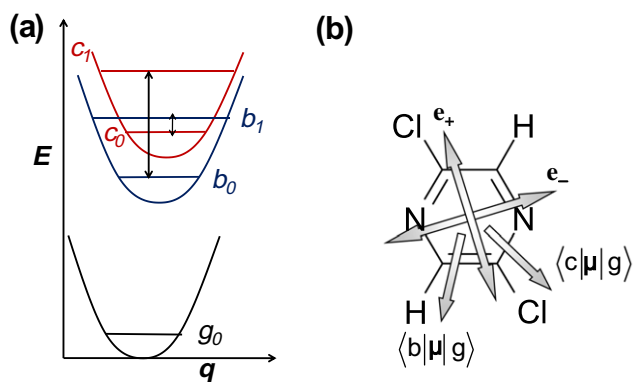

Fig. 1. (a) A simplified model for a nonadiabatic interaction between coherently excited quasi-degenerate vibronic states. (b) Photon polarization directions for control of relative phases between the nearly degenerate electronic states. The directions of e_+ and e_- are defined as $\mu_{bg} \bullet e_+ = \mu_{cg} \bullet e_+$ and $\mu_{bg} \bullet e_- = -\mu_{cg} \bullet e_-$, respectively.

(DCP) in Fig. 1b [7]. In Fig. 1a, q denotes the dimensionless normal coordinate of the breathing mode [11]. The potentials in the ground and two electronic excited states (b and c) were assumed to be displaced and undistorted ones. At least two vibrational eigenstates in each electronic state are needed for consideration of both the electronic and vibrational coherences in the simplified model. Here, $b0$ ($c0$) and $b1$ ($c1$) denote the lowest and the first excited vibrational eigenstates belonging to the b (c) quasi-degenerate electronic state.

The relative phase between two electronic states, b and c, can be controlled by changing the directions of the polarization unit vectors e_+ and e_- of linearly polarized laser pulses as shown in Fig. 1b [7]. The directions of e_+ and e_- are defined as $\mu_{bg} \bullet e_+ = \mu_{cg} \bullet e_+$ and $\mu_{bg} \bullet e_- = -\mu_{cg} \bullet e_-$, respectively. Here, the transition moment vector for an optical transition from the ground state g to the lower electronic state b, $\mu_{bg} \equiv \langle b \mid \mu \mid g \rangle$, and that to the higher electronic state c, $\mu_{cg} \equiv \langle c \mid \mu \mid g \rangle$ where μ is the electric dipole moment are on the aromatic – ring plane and almost orthogonal to each other because of small differences in energy between the two electronic excited states b and c.

The time evolution of the quantum system in the low temperature limit can be expressed as

$$\Psi(t) = c_{g0}(t)|\Phi_g X_{g0}\rangle + c_{c1}(t)|\Phi_c X_{c1}\rangle + c_{c0}(t)|\Phi_c X_{c0}\rangle$$
$$+ \eta(c_{b0}(t)|\Phi_b X_{b0}\rangle + c_{b1}(t)|\Phi_b X_{b1}\rangle). \quad (1)$$

Here, Φ and X denote the electronic and vibrational wavefunctions, respectively.

Time-dependent coefficients $c(t)$ are obtained by solving the time-dependent Schrödinger equation,

$$i\hbar\frac{\partial}{\partial t}|\Psi(t)\rangle = (\hat{H}_0 + \hat{V} + U(t))|\Psi(t)\rangle. \quad (2)$$

Here, $\hat{H}_0$ is the molecular Hamiltonian in the Born–Oppenheimer approximation, and $\hat{V}$ is the nonadiabatic coupling operator. $U(t) = \mu \cdot E(t)\cos(\omega_L t)$ is the pulse excitation operator. Here, $E(t)$ is the amplitude of the laser pulse with photon-polarization vector e and ω_L is laser central frequency.

In Eq. (1), η denotes the parameter depending on photon polarization direction of the linearly polarized laser pulse: $\eta = 1$ for the polarization vector e_+, while $\eta = -1$ for e_-.

The nonadiabatically coupled system shown in Fig. 1 consists of two nonadiabatic transition processes: one is $c1 \leftrightarrow b0$ and the other is $c0 \leftrightarrow b1$. Other processes, $c0 \leftrightarrow b0$ and $c1 \leftrightarrow b1$ were omitted. This is because the nonadiabatic coupling matrix elements between the two vibronic states with the equal vibrational quantum number approximately give zero for the displaced harmonic potential model with dimensionless potential displacement $|\Delta_{cb}| \ll 1$.

First, consider nonadiabatic transition processes $c1 \leftrightarrow b0$. In this section, we derive analytical expressions for temporal behaviors of the electronic and vibrational coherences by focusing on the nonadiabatic coupling effects. For this purpose, we set the initial condition as $c_{g0}(0) = 0$, $c_{b0}(0) \neq 0$ and $c_{c1}(0) \neq 0$, omitting the pulse excitation effects. In the results and discussion section, we take into account both the nonadiabatic effects and pulse excitation effects to compare the temporal behaviors obtained in the simplified model and those in the nuclear wavepacket simulation.

The dynamical behaviors can be obtained by solving the following coupled equation:

$$i\hbar\frac{\partial}{\partial t}\begin{pmatrix} c_{c1}(t) \\ c_{b0}(t) \end{pmatrix} = \begin{pmatrix} E_{c1} & \eta V_{c1,b0} \\ \eta V_{b0,c1} & E_{b0} \end{pmatrix}\begin{pmatrix} c_{c1}(t) \\ c_{b0}(t) \end{pmatrix}. \quad (3)$$

Here, $V_{c1,b0}$ is the nonadiabatic coupling matrix element between vibronic state $c1$ with energy E_{c1} and vibronic state $b0$ with energy E_{b0}. In the displaced and undistorted potential model,

$E_{b1} - E_{b0} = E_{c1} - E_{c0}$ is satisfied. The solution is given by solving the equation

$$\begin{pmatrix} E_{c1} - \lambda & \eta V_{c1,b0} \\ \eta V_{b0,c1} & E_{b0} - \lambda \end{pmatrix} \begin{pmatrix} A \\ A' \end{pmatrix} = 0. \tag{4}$$

A general solution can be expressed as

$$\begin{pmatrix} c_{c1}(t) \\ c_{b0}(t) \end{pmatrix} = \begin{pmatrix} A_1 e^{\frac{i\lambda_1 t}{\hbar}} \\ A_1' e^{-\frac{i\lambda_1 t}{\hbar}} \end{pmatrix} + \begin{pmatrix} A_2 e^{\frac{i\lambda_2 t}{\hbar}} \\ A_2' e^{-\frac{i\lambda_2 t}{\hbar}} \end{pmatrix} \tag{5}$$

with λ's

$$\lambda_1 = E^0_{c1,b0} - \frac{\gamma_{c1,b0}}{2}; \quad \lambda_2 = E^0_{c1,b0} + \frac{\gamma_{c1,b0}}{2}, \tag{6a}$$

where

$$E^0_{c1,b0} = \frac{E_{c1} + E_{b0}}{2}, \tag{6b}$$

$$\gamma_{c1,bo} = \sqrt{(\Delta E_{c1,b0})^2 + 4|V_{c1,b0}|^2}, \tag{6c}$$

and

$$\Delta E_{c1,b0} = E_{c1} - E_{b0}. \tag{6d}$$

A's are determined using both Eq. (4) and the initial condition

$$\begin{pmatrix} c_{c1}(0) \\ c_{b0}(0) \end{pmatrix} = \begin{pmatrix} A_1 \\ A_1' \end{pmatrix} + \begin{pmatrix} A_2 \\ A_2' \end{pmatrix}. \tag{7}$$

Here, each coefficient can be expressed as

$$A_1 = \frac{\frac{(\gamma_{c1,b0} - \Delta E_{c1,b0})}{2} c_{c1}(0) - \eta V_{c1,b0} c_{b0}(0)}{\gamma_{c1,b0}}, \tag{8a}$$

$$A_1' = \frac{-\eta V_{c1,b0} c_{c1}(0) + \frac{(\gamma_{c1,b0} + \Delta E_{c1,b0})}{2} c_{b0}(0)}{\gamma_{c1,b0}}, \tag{8b}$$

$$A_2 = \frac{\frac{(\gamma_{c1,b0} + \Delta E_{c1,b0})}{2} c_{c1}(0) + \eta V_{c1,b0} c_{b0}(0)}{\gamma_{c1,b0}}, \tag{8c}$$

and

$$A_2' = \frac{\eta V_{c1,b0} c_{c1}(0) + \frac{(\gamma_{c1,b0} - \Delta E_{c1,b0})}{2} c_{b0}(0)}{\gamma_{c1,b0}}. \tag{8d}$$

Finally, the time-dependent coefficients for $c1 \leftrightarrow b0$ can be expressed as

$$\begin{pmatrix} c_{c1}(t) \\ c_{b0}(t) \end{pmatrix} = \frac{1}{\gamma_{c1,b0}} \begin{pmatrix} \left\{ \frac{(\gamma_{c1,b0} - \Delta E_{c1,b0})}{2} c_{c1}(0) - \eta V_{c1,b0} c_{b0}(0) \right\} \exp\left[-\frac{i\lambda_1 t}{\hbar} \right] \\ \left\{ -\eta V_{c1,b0} c_{c1}(0) + \frac{(\gamma_{c1,b0} + \Delta E_{c1,b0})}{2} c_{b0}(0) \right\} \exp\left[-\frac{i\lambda_1 t}{\hbar} \right] \end{pmatrix}$$
$$+ \frac{1}{\gamma_{c1,b0}} \begin{pmatrix} \left\{ \frac{(\gamma_{c1,b0} + \Delta E_{c1,b0})}{2} c_{c1}(0) + \eta V_{c1,b0} c_{b0}(0) \right\} \exp\left[-\frac{i\lambda_2 t}{\hbar} \right] \\ \left\{ \eta V_{c1,b0} c_{c1}(0) + \frac{(\gamma_{c1,b0} - \Delta E_{c1,b0})}{2} c_{b0}(0) \right\} \exp\left[-\frac{i\lambda_2 t}{\hbar} \right] \end{pmatrix}. \tag{9}$$

Next, consider nonadiabatic transition processes $c0 \leftrightarrow b1$ in the same procedure that as described above. The dynamical behaviors can be obtained by solving the coupled equation:

$$i\hbar \frac{\partial}{\partial t} \begin{pmatrix} c_{c0}(t) \\ c_{b1}(t) \end{pmatrix} = \begin{pmatrix} E_{c0} & \eta V_{c0,b1} \\ \eta V_{b1,c0} & E_{b1} \end{pmatrix} \begin{pmatrix} c_{c0}(t) \\ c_{b1}(t) \end{pmatrix}. \tag{10}$$

Here, $V_{c0,b1}$ is the nonadiabatic coupling matrix element between the two vibronic excited states $c0$ and $b1$. The solution of Eq. (10) can be obtained as

$$\begin{pmatrix} c_{c0}(t) \\ c_{b1}(t) \end{pmatrix} = \frac{1}{\gamma_{c0,b1}} \begin{pmatrix} \left\{ \frac{(\gamma_{c0,b1} - \Delta E_{c0,b1})}{2} c_{c0}(0) - \eta V_{c0,b1} c_{b1}(0) \right\} \exp\left[-\frac{i\kappa_1 t}{\hbar} \right] \\ \left\{ -\eta V_{c0,b1} c_{c0}(0) + \frac{(\gamma_{c0,b1} + \Delta E_{c0,b1})}{2} c_{b1}(0) \right\} \exp\left[-\frac{i\kappa_1 t}{\hbar} \right] \end{pmatrix}$$
$$+ \frac{1}{\gamma_{c0,b1}} \begin{pmatrix} \left\{ \frac{(\gamma_{c0,b1} + \Delta E_{c0,b1})}{2} c_{c0}(0) + \eta V_{c0,b1} c_{b1}(0) \right\} \exp\left[-\frac{i\kappa_2 t}{\hbar} \right] \\ \left\{ \eta V_{c0,b1} c_{c0}(0) + \frac{(\gamma_{c0,b1} - \Delta E_{c0,b1})}{2} c_{b1}(0) \right\} \exp\left[-\frac{i\kappa_2 t}{\hbar} \right] \end{pmatrix}. \tag{11}$$

Here,

$$\kappa_1 = E^0_{c0,b1} - \frac{\gamma_{c0,b1}}{2}, \quad \kappa_2 = E^0_{c0,b1} + \frac{\gamma_{c0,b1}}{2}, \tag{12a}$$

$$E^0_{c0,b1} = \frac{E_{c0} + E_{b1}}{2}, \tag{12b}$$

$$\gamma_{c0,b1} = \sqrt{(\Delta E_{c0,b1})^2 + 4|V_{c0,b1}|^2}, \tag{12c}$$

and

$$\Delta E_{c0,b1} \equiv E_{c0} - E_{b1}. \tag{12d}$$

3. Results and discussion

In this section, based on the analytical expressions for time evolution of nuclear dynamics of nonadiabatically coupled quasi-degenerate electronic states, we discuss two issues, the photon polarization-dependent population in each vibronic state and vibrational coherence transfer between the two electronic states through nonadiabatic couplings.

3.1. Photon polarization-dependent populations

The time evolution of populations of two vibronic states, $c1$ and $b0$, can be expressed by using Eqs. (9) and (11) as

$$\rho_{c1,c1}(t) = \frac{1}{\gamma^2_{c1,b0}} \left[\frac{\left(\gamma^2_{c1,b0} + \Delta E^2_{c1,b0} \right)}{2} c_{c1}(0)^2 + 2V^2_{c1,b0} c_{b0}(0)^2 \right.$$
$$+ 2\eta V_{c1,b0} \Delta E_{c1,b0} c_{c1}(0) c_{b0}(0)$$
$$+ \left\{ \frac{\left(\gamma^2_{c1,b0} - \Delta E^2_{c1,b0} \right)}{2} c_{c1}(0)^2 - 2V^2_{c1,b0} c_{b0}(0)^2 \right.$$
$$\left. - 2\eta V_{c1,b0} \Delta E_{c1,b0} c_{c1}(0) c_{b0}(0) \right\} \cos\left(\frac{\gamma_{c1,b0}}{\hbar} t \right) \right], \tag{13a}$$

and

$$\rho_{b0,b0}(t) = \frac{1}{\gamma^2_{c1,b0}} \left[\frac{\left(\gamma^2_{c1,b0} + \Delta E^2_{c1,b0} \right)}{2} c_{b0}(0)^2 + 2V^2_{c1,b0} c_{c1}(0)^2 \right.$$
$$- 2\eta V_{c1,b0} \Delta E_{c1,b0} c_{b0}(0) c_{c1}(0)$$
$$+ \left\{ \frac{\left(\gamma^2_{c1,b0} - \Delta E^2_{c1,b0} \right)}{2} c_{b0}(0)^2 - 2V^2_{c1,b0} c_{c1}(0)^2 \right.$$
$$\left. + 2\eta V_{c1,b0} \Delta E_{c1,b0} c_{b0}(0) c_{c1}(0) \right\} \cos\left(\frac{\gamma_{c1,b0}}{\hbar} t \right) \right], \tag{13b}$$

respectively. In a similar way, $\rho_{c0,c0}(t)$ and $\rho_{b1,b1}(t)$ can be expressed.

For simplicity, consider temporal behaviors in which all of the initial vibronic states are equally distributed, i. e., $c_{c1}(0) = c_{b0}(0) = c(0)$. For this case, Eqs. (13a) and (13b) are simplified as

$$\rho_{c1,c1}(t) = c(0)^2 \left[1 + \frac{2\eta V_{c1,b0} \Delta E_{c1,b0}}{\gamma_{c1,b0}^2} \left\{ 1 - \cos\left(\frac{\gamma_{c1,b0}}{h}t\right) \right\} \right], \quad (14a)$$

and

$$\rho_{b0,b0}(t) = c(0)^2 \left[1 - \frac{2\eta V_{c1,b0} \Delta E_{c1,b0}}{\gamma_{c1,b0}^2} \left\{ 1 - \cos\left(\frac{\gamma_{c1,b0}}{h}t\right) \right\} \right], \quad \text{respectively.}$$
$$(14b)$$

It can be seen from Eqs. (14) that temporal behaviors of populations depend on the phase of $\eta V_{c1,b0} \Delta E_{c1,b0}$, i.e., that of $\eta V_{c1,b0}$ since $\Delta E_{c1,b0} > 0$. We call $\eta V_{c1,b0}$ phase parameter in this paper. This parameter determines constructive or destructive interference between the two vibronic states. For the upper vibronic state, a positive value of the parameter gives constructive interference, and it increases in the population at the initial stage before the reversible process takes place, while for the lower vibronic state, it gives destructive interference and decreases in the population.

Fig. 2a shows the results of calculated time evolution of the two vibronic states; the solid line denotes $\rho_{b0,b0}(t)$ and the broken line denotes $\rho_{c1,c1}(t)$. Here, $\eta V_{c1,b0} > 0$ was adopted for the phase parameter. Values of the parameters used were $|V_{c1,b0}| = 0.025$ eV as the magnitude of the nonadiabatic coupling matrix element, $\Delta E_{c1,b0} = 0.225$ eV and $\Delta E_{c0,b1} = -0.075$ eV as the energy differences between the two vibronic states for the nonadiabatic transition process. These parameters were taken from the results for potential energy surfaces of 2,5-dichloropyrazine, which were calculated by an *ab initio* MO method [12]. Here, *ab initio* geometry optimization for the ground state was carried out using MOLPRO [13] at the MP2/6-31G* level followed by a single-point ground- and excited-state calculation at the CASSCF(10,8)/6-31G* level. The relation between the two nonadiabatic coupling matrix elements, $V_{c0,b1} = -V_{c1,b0}$, was used [14]. The oscillation in Fig. 2a indicates the population transfer between c and b electronic excited states with recurrence time of $\tau_{rec} = 2\pi\hbar/\gamma_{c1,b0} = 18.3$ fs.

Fig. 2b shows the population changes taking into account effects of pulse excitation in order to make comparison with the temporal behaviors obtained in the nuclear wavepacket simulation. The wavepacket simulation was carried out on the multidimensional potential surfaces calculated by *ab initio* MO method [7]. The effects of the nonadiabatic coupling were obtained by numerically solving the coupled equations with the split-operator method for the multidimensional surface Hamiltonian, and the resultant diabatic wavepackets were converted to adiabatic wavepackets [7]. The amplitude of the laser pulse used $E(t)$ was drown by the dotted line in Fig. 2b. The four vibronic states are coherently excited by the pulse. The same molecular parameter set as that used in Fig. 2a was used. It can be seen from Fig. 2b that the analytical results reproduce the photon polarization-dependent dynamic behaviors that appeared in the nuclear wavepacket simulation, especially at the early time regime before one cycle of the oscillation. This indicates that the simplified model used in this paper is valid to explain the characteristic features and that the photon polarization-dependent populations originate from the interference between the two coherently excited vibronic states. After the early time regime, the time evolution of the populations calculated using the simplified model deviate from those obtained in the nuclear wavepacket simulation because effects due to vibrational mode couplings, which was neglected in the simplified model, may make a significant contribution.

The coherent dynamics are reversible since the system is isolated and there are no bath modes in our simplified one-dimensional model. Therefore, if the two electronic states are coherently excited by a linearly polarized pulse, the dynamic behaviors are invariant with respect to change in the direction of polarization, $\eta = 1$ (e_+) or $\eta = -1$ (e_-). Time-dependent behaviors of $\rho_{c1,c1}(t)$ with
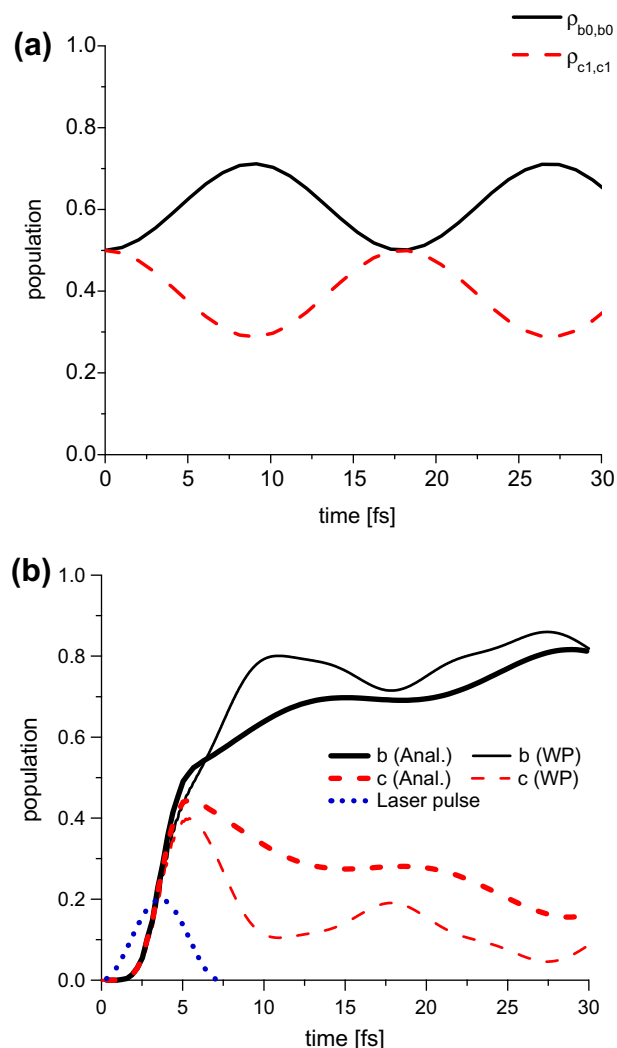

Fig. 2. Photon polarization-dependent populations as a function of time. In (a), the solid line denotes $\rho_{b0,b0}(t)$ and the broken line denotes $\rho_{c1,c1}(t)$, which were calculated with the analytical expressions for $\eta V_{c1,b0} > 0$ with $\eta = -1$. The parameter sets used are $|V_{c1,b0}| = 0.025$ eV, $\Delta E_{c1,b0} = 0.225$ eV and $\Delta E_{c0,b1} = -0.075$ eV. In (b), the bold solid line denotes the population in lower electronic state b, $\rho_{b,b}(t) = \rho_{b0,b0}(t) + \rho_{b1,b1}(t)$ that are obtained by using the analytical expressions, and the bold broken line denotes the population in upper electronic state c, $\rho_{c,c}(t) = \rho_{c0,c0}(t) + \rho_{c1,c1}(t)$ that are obtained by using the analytical expressions, for $\eta V_{c1,b0} > 0$ with $\eta = -1$. An excitation process from the ground state was taken into account for comparison with the results of wavepacket simulations [7] (thin solid (broken) line for the population in b (c)). The envelope of the pulse used was $A \sin^2\left(\frac{\pi t}{\tau_p}\right)$ with $A = 6.50 \times 10^9$ V/m and $\tau_p = 7.26$ fs, which is denoted by a dotted line.

e_+ (e_-) is the same as $\rho_{b0,b0}(t)$ with $\eta = -1$ ($\eta = 1$). In real molecules with many vibrational degrees of freedom, the invariance is broken and dephasing time of the vibrational coherence in lower excited state b is shorter than that in higher state c because multimode effects induced by potential couplings and/or an harmonicity play a much more dominant role in lower state b than in higher state c.

3.2. Vibrational coherence transfer through nonadiabatic couplings

The vibrational coherence between $c1$ and $c0$ states in electronic state c, $\rho_{c1,c0}(t)$, is expressed using Eqs. (9) and (11) as

$$\rho_{c1,c0}(t) = \text{Re}\,\rho_{c1,c0}(t) + i\,\text{Im}\,\rho_{c1,c0}(t), \quad (15)$$

where

$$\text{Re}\rho_{c1,c0}(t) = \frac{1}{\gamma_{c1,b0}\gamma_{c0,b1}}\left[\frac{1}{2}(\gamma_{c1,b0}\gamma_{c0,b1} + \Delta E_{c1,b0}\Delta E_{c0,b1})c_{c1}(0)c_{c0}(0)\right.$$
$$+ \eta(\Delta E_{c0,b1}V_{c1,b0}c_{b0}(0)c_{c0}(0) + \Delta E_{c1,b0}V_{c0,b1}c_{b1}(0)c_{c1}(0))$$
$$\left.+ 2V_{c1,b0}V_{c0,b1}c_{b1}(0)c_{b0}(0)\right]\cos\left[\frac{(\gamma_{c1,b0} - \gamma_{c0,b1})}{2\hbar}t\right]$$
$$+ \frac{1}{\gamma_{c1,b0}\gamma_{c0,b1}}\left[\frac{1}{2}(\gamma_{c1,b0}\gamma_{c0,b1} - \Delta E_{c1,b0}\Delta E_{c0,b1})c_{c1}(0)c_{c0}(0)\right.$$
$$- \eta(\Delta E_{c0,b1}V_{c1,b0}c_{b0}(0)c_{c0}(0) + \Delta E_{c1,b0}V_{c0,b1}c_{b1}(0)c_{c1}(0))$$
$$\left.- 2V_{c1,b0}V_{c0,b1}c_{b1}(0)c_{b0}(0)\right]\cos\left[\frac{(\gamma_{c1,b0} + \gamma_{c0,b1})}{2\hbar}t\right],$$
$$(16a)$$

and

$$\text{Im}\rho_{c1,c0}(t) = -\frac{1}{\gamma_{c1,b0}\gamma_{c0,b1}}\left[\frac{1}{2}(\gamma_{c1,b0}\Delta E_{c0,b1} + \gamma_{c0,b1}\Delta E_{c1,b0})c_{c1}(0)c_{c0}(0)\right.$$
$$\left.+ \eta(V_{c1,b0}\gamma_{c0,b1}c_{b0}(0)c_{c0}(0) + V_{c0,b1}\gamma_{c1,b0}c_{c1}(0)c_{b1}(0))\right]$$
$$\times \sin\left[\frac{(\gamma_{c0,b1} - \gamma_{c1,b0})}{2\hbar}t\right]$$
$$- \frac{1}{\gamma_{c1,b0}\gamma_{c0,b1}}\left[\frac{1}{2}(\gamma_{c1,b0}\Delta E_{c0,b1} - \gamma_{c0,b1}\Delta E_{c1,b0})c_{c1}(0)c_{c0}(0)\right.$$
$$\left.+ \eta(\gamma_{c1,b0}V_{c0,b1}c_{b1}(0)c_{c1}(0) - \gamma_{c0,b1}V_{c1,b0}c_{b0}(0)c_{c0}(0))\right]$$
$$\times \sin\left[\frac{(\gamma_{c1,b0} + \gamma_{c0,b1})}{2\hbar}t\right].$$
$$(16b)$$

In a similar way, the vibrational coherence between the two vibronic states, $b1$ and $b0$ in electronic state b, $\rho_{b1,b0}(t)$, can be expressed as

$$\rho_{b1,b0}(t) = \text{Re}\rho_{b1,b0}(t) + i\text{Im}\rho_{b1,b0}(t), \tag{17}$$

where

$$\text{Re}\rho_{b1,b0}(t) = \frac{1}{\gamma_{c1,b0}\gamma_{c0,b1}}\left[\frac{1}{2}(\gamma_{c1,b0}\gamma_{c0,b1} + \Delta E_{c1,b0}\Delta E_{c0,b1})c_{b1}(0)c_{b0}(0)\right.$$
$$- \eta(\Delta E_{c0,b1}V_{c1,b0}c_{b1}(0)c_{c1}(0) + \Delta E_{c1,b0}V_{c0,b1}c_{b0}(0)c_{c0}(0))$$
$$\left.+ 2V_{c1,b0}V_{c0,b1}c_{c1}(0)c_{c0}(0)\right]\cos\left[\frac{(\gamma_{c1,b0} - \gamma_{c0,b1})}{2\hbar}t\right]$$
$$+ \frac{1}{\gamma_{c1,b0}\gamma_{c0,b1}}\left[\frac{1}{2}(\gamma_{c1,b0}\gamma_{c0,b1} - \Delta E_{c1,b0}\Delta E_{c0,b1})c_{b1}(0)c_{b0}(0)\right.$$
$$+ \eta(\Delta E_{c0,b1}V_{c1,b0}c_{b1}(0)c_{c1}(0) + \Delta E_{c1,b0}V_{c0,b1}c_{b0}(0)c_{c0}(0))$$
$$\left.- 2V_{c1,b0}V_{c0,b1}c_{c1}(0)c_{c0}(0)\right]\cos\left[\frac{(\gamma_{c1,b0} + \gamma_{c0,b1})}{2\hbar}t\right]$$
$$(18a)$$

and

$$\text{Im}\rho_{b1,b0}(t) = -\frac{1}{\gamma_{c1,b0}\gamma_{c0,b1}}\left[\frac{1}{2}(\gamma_{c0,b1}\Delta E_{c1,b0} + \gamma_{c1,b0}\Delta E_{c0,b1})c_{b1}(0)c_{b0}(0)\right.$$
$$\left.- \eta(\gamma_{c0,b1}V_{c1,b0}c_{b1}(0)c_{c1}(0) + \gamma_{c1,b0}V_{c0,b1}c_{b0}(0)c_{c0}(0))\right]$$
$$\times \sin\left[\frac{(\gamma_{c0,b1} - \gamma_{c1,b0})}{2\hbar}t\right]$$
$$- \frac{1}{\gamma_{c1,b0}\gamma_{c0,b1}}\left[\frac{1}{2}(\gamma_{c1,b0}\Delta E_{c0,b1} - \gamma_{c0,b1}\Delta E_{c1,b0})c_{b1}(0)c_{b0}(0)\right.$$
$$\left.- \eta(V_{c0,b1}\gamma_{c1,b0}c_{b0}(0)c_{c0}(0) - V_{c1,b0}\gamma_{c0,b1}c_{b1}(0)c_{c1}(0))\right]$$
$$\times \sin\left[\frac{(\gamma_{c0,b1} + \gamma_{c1,b0})}{2\hbar}t\right].$$
$$(18b)$$

We consider a simplified case in which all of the vibronic states are equally distributed at $t = 0$, i.e., $c_{c0}(0) = c_{c1}(0) = c_{b0}(0) = c_{b1}(0) \equiv c(0)$. In this case, Eqs. (16a) and (18a) are simplified as

$$\text{Re}\rho_{c1,c0}(t) = c(0)^2\left[\cos\left(\frac{\gamma_{c1,b0}t}{2\hbar}\right)\cos\left(\frac{\gamma_{c0,b1}t}{2\hbar}\right)\right.$$
$$+ \left\{\frac{\Delta E_{c1,b0}}{\gamma_{c1,b0}}\frac{\Delta E_{c0,b1}}{\gamma_{c0,b1}} + 2\frac{V_{c1,b0}}{\gamma_{c1,b0}}\frac{V_{c0,b1}}{\gamma_{c0,b1}}\right.$$
$$\left.+ \eta\left(\frac{\Delta E_{c0,b1}}{\gamma_{c0,b1}}\frac{V_{c1,b0}}{\gamma_{c1,b0}} + \frac{\Delta E_{c1,b0}}{\gamma_{c1,b0}}\frac{V_{c0,b1}}{\gamma_{c0,b1}}\right)\right\}\sin\left(\frac{\gamma_{c1,b0}t}{2\hbar}\right)$$
$$\left.\times \sin\left(\frac{\gamma_{c0,b1}t}{2\hbar}\right)\right], \tag{19a}$$

and

$$\text{Re}\rho_{b1,b0}(t) =]c(0)^2\left[\cos\left(\frac{\gamma_{c1,b0}t}{2\hbar}\right)\cos\left(\frac{\gamma_{c0,b1}t}{2\hbar}\right)\right.$$
$$+ \left\{\frac{\Delta E_{c1,b0}}{\gamma_{c1,b0}}\frac{\Delta E_{c0,b1}}{\gamma_{c0,b1}} + 2\frac{V_{c1,b0}}{\gamma_{c1,b0}}\frac{V_{c0,b1}}{\gamma_{c0,b1}}\right.$$
$$\left.- \eta\left(\frac{\Delta E_{c0,b1}}{\gamma_{c0,b1}}\frac{V_{c1,b0}}{\gamma_{c1,b0}} + \frac{\Delta E_{c1,b0}}{\gamma_{c1,b0}}\frac{V_{c0,b1}}{\gamma_{c0,b1}}\right)\right\}\sin\left(\frac{\gamma_{c1,b0}t}{2\hbar}\right)$$
$$\left.\times \sin\left(\frac{\gamma_{c0,b1}t}{2\hbar}\right)\right], \tag{19b}$$

respectively.

Fig. 3 shows the results for temporal behaviors of vibrational coherences, which were calculated by using Eqs. (19). Here, the same values for nonadiabatic coupling matrix elements and energy differences as those in Fig. 2 were adopted. In Fig. 3a, temporal behaviors for $\eta = -1$ are presented. The solid line and broken line denote $\text{Re}\rho_{c1,c0}(t)$ and $\text{Re}\rho_{b1,b0}(t)$, respectively. It can be seen that the phase of $\text{Re}\rho_{c1,c0}(t)$ and that of $\text{Re}\rho_{b1,b0}(t)$ in the initial stage are the same, although their magnitudes are different. The differences in the magnitude come from the interference effects: constructive interference for $\text{Re}\rho_{c1,c0}(t)$, while destructive interference for $\text{Re}\rho_{b1,b0}(t)$. The vibrational coherence transfers considered here are also reversible as the population transfers. That is, for polarization behaviors $\text{Re}\rho_{c1,c0}(t)$ with $\eta = 1$ ($\eta = -1$) is the same as $\text{Re}\rho_{b1,b0}(t)$ with $\eta = -1$ ($\eta = 1$).

We now consider the simplest case in which optical excitation is allowed to the electronic excited state c, i.e., $\mu_{cg} \neq 0$ and $c_{c0}(0) = c_{c1}(0) \equiv c(0) \neq 0$, but is forbidden to the lower state b, i.e., b is a dark state, $\mu_{bg} = 0$ and $c_{b0}(0) = c_{b1}(0) = 0$.

The quantum beat signal due to formation of vibrational coherence in excited electronic state c is proportional to

$$\text{Re}\rho_{c1,c0}(t) = c(0)^2\left[\cos\left(\frac{\gamma_{c1,b0}t}{2\hbar}\right)\cos\left(\frac{\gamma_{c0,b1}t}{2\hbar}\right)\right.$$
$$\left.+ \frac{\Delta E_{c1,b0}\Delta E_{c0,b1}}{\gamma_{c1,b0}\gamma_{c0,b1}}\sin\left(\frac{\gamma_{c1,b0}t}{2\hbar}\right)\sin\left(\frac{\gamma_{c0,b1}t}{2\hbar}\right)\right], \tag{20a}$$

while the quantum beat signal in state b, which originated from the vibrational coherence transferred through nonadiabatic coupling is proportional to

$$\text{Re}\rho_{b1,b0}(t) = 4c(0)^2\frac{V_{c1,b0}V_{c0,b1}}{\gamma_{c1,b0}\gamma_{c0,b1}}\sin\left(\frac{\gamma_{c1,b0}}{2\hbar}t\right)\sin\left(\frac{\gamma_{c0,b1}}{2\hbar}t\right). \tag{20b}$$

We now discuss the quantum beat frequencies. For $\Delta E_{c1,b0} \gg V_{c1,b0}$ and $|\Delta E_{c0,b1}| \gg |V_{c0,b1}|$, Eq. (20a) can be reduced to

$$\text{Re}\rho_{c1,c0}(t) \approx c(0)^2\cos(\omega t). \tag{21a}$$

Here, $\omega \equiv \frac{\Delta E_{c1,b0} - \Delta E_{c0,b1}}{2\hbar} = \frac{E_{c1} - E_{c0}}{\hbar}$, which is equal to the vibrational frequency relevant to the vibrational coherence transfer. Equation (21a) simply reveals that the beat frequency originates from the vibrational coherence created in state c.
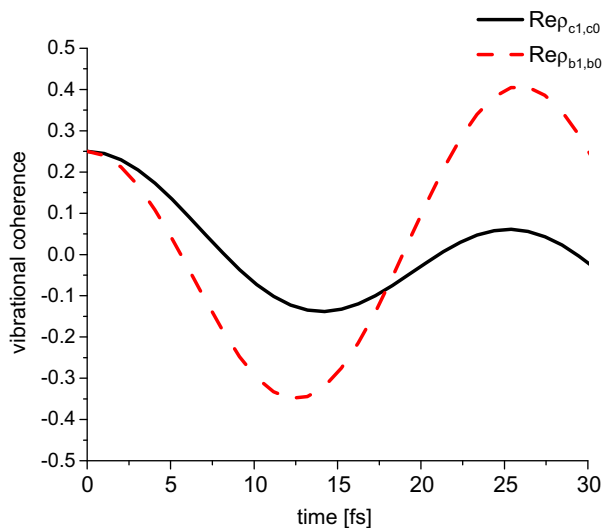
In a similar way, Eq. (20b) can be reduced to

Fig. 3. Photon polarization-dependent vibrational coherences as a function of time. $\mathrm{Re}\rho_{c1,c0}(t)$ is denoted by a solid line and $\mathrm{Re}\rho_{b1,b0}(t)$ is denoted by a broken line. The same parameter set as that in Fig. 2 was adopted.

Fig. 4. Vibrational coherences as a function of time, $\rho_{c1,c0}(t)$ and $\rho_{b1,b0}(t)$ in the case in which the initial vibrational coherence is created on the upper excited state c. The same parameter set as that in Fig. 2 was adopted.

$$\mathrm{Re}\rho_{b1,b0}(t) \approx 2c(0)^2 \frac{V_{c1,b0}V_{c0,b1}}{\gamma_{c1,b0}\gamma_{c0,b1}} \{\cos(\omega t) - \cos(\bar{\omega}t)\}. \tag{21b}$$

Here, $\bar{\omega} \equiv \frac{\Delta E_{c1,b0}+\Delta E_{c0,b1}}{2\hbar} = \frac{\Delta E_{cb}}{\hbar}$, which is equal to the transition frequency between the two electronic states, c and b: $\Delta E_{cb} \equiv E_{c0} - E_{b0}$ or $(E_{c1} - E_{b1})$.

The frequencies relevant to the transferred vibrational coherence consist of two components: one is the vibrational frequency relevant to the vibrational coherence transfer, and the other is the transition frequency. The latter originates from the generation of vibronic coherences as the intermediate processes in the course of the vibrational coherence transfer.

We next discuss the amplitudes of the quantum beats. The ratio of beat amplitudes between two vibrational coherences can be approximately expressed at $t = (2n+1)\pi\hbar/\gamma_{c1,b0}$ or $t = (2n+1)\pi\hbar/\gamma_{c0,b1}$ with $n = 0, 1, 2, \ldots$ as

$$\left|\frac{\mathrm{Re}\rho_{b1,b0}(t)}{\mathrm{Re}\rho_{c1,c0}(t)}\right| \approx \left|\frac{2V_{c1,b0}}{\Delta E_{c1,b0}}\right|\left|\frac{2V_{c0,b1}}{\Delta E_{c0,b1}}\right|. \tag{22}$$

Equation (22) indicates that the ratio of beat amplitudes between the two quantum beats before and after transfer through nonadiabatic couplings is given by the products of the individual ratios of the nonadiabatic coupling matrix element to the corresponding energy difference. In other words, information on the nonadiabatic transition can be evaluated by analyzing the beat signals. Equation (22) can be roughly expressed as

$$\left|\frac{\mathrm{Re}\rho_{b1,b0}(t)}{\mathrm{Re}\rho_{c1,c0}(t)}\right| \approx \left|\frac{2\bar{V}}{\Delta\bar{E}}\right|^2. \tag{23}$$

Here, $\bar{V}$ denotes the averaged nonadiabatic coupling matrix element relevant to the transition process and $\Delta\bar{E}(= \hbar\bar{\omega})$ is the corresponding averaged energy difference.

This indicates that not only the energy difference but also the nonadiabatic coupling matrix element can be determined by analyzing the beat signals, i.e., the beat frequencies and amplitudes. The results are in contrast to those of ordinary quantum beat experiments [15]. Only energy differences between coherently excited eigenstates are observed in ordinary quantum beat experiments.

Fig. 4 shows an example of temporal behaviors of vibrational coherences, which were calculated by using Eq. (20). Here, the same values of the parameters as those used in Fig. 3 were
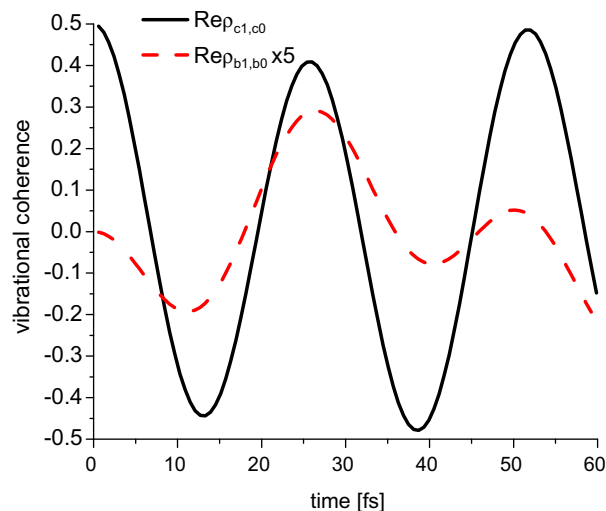
adopted. The solid line and dotted line denote $\mathrm{Re}\rho_{c1,c0}(t)$ and $\mathrm{Re}\rho_{b1,b0}(t)$, respectively. The magnitude of $\mathrm{Re}\rho_{c1,c0}(t)$ was drawn by multiplying the original magnitude by five. The ratio of the magnitudes is given by 0.06.

Recently, Suzuki et al. [4] reported quantum beats in time-resolved photoelectron spectra after ultrafast internal conversion from the optically active $\pi\pi^*$ electronic excited state of pyrazine in vapor. Mechanisms of ultrafast nonradiative decay processes of pyrazine have been actively investigated [16–18]. Results of our theoretical study on the vibrational coherence transfer through nonadiabatic couplings suggest that detailed information on the dark electronic states associated with the ultrafast internal conversion can be obtained by analyzing the two quantum beats before and after coherence transfer through nonadiabatic couplings.

4. Conclusion

In this paper, we presented the results of theoretical study on ultrafast coherent nuclear dynamics of nonadiabatically coupled quasi-degenerate electronic excited states of an aromatic molecule. Analytical expressions for time-dependent populations and vibrational coherences were derived for a simple, one-dimensional model. It was demonstrated that the polarization-dependent populations found by nuclear wavepacket simulations originate from the interferences between the two quasi-degenerate electronic states coherently excited by a femtosecond laser pulse. Another coherent dynamics, vibrational coherence transfer through nonadiabatic couplings was clarified: structures of the beat signal and amplitudes of vibrational coherence transfer were derived. It was shown that both the energy difference and the nonadiabatic coupling matrix element can be obtained by analyzing the two quantum beat signals before and after the transfer through nonadiabatic couplings.

References

[1] G.S. Engel, T.R. Calhoun, E.L. Read, T.-K. Ahn, T. Mančal, Y.-C. Cheng, R.E. Blankenship, G.R. Fleming, Nature 446 (2007) 782.

[2] E. Collini, G.D. Scholes, Science 323 (2009) 369.

[3] S. Takeuchi, S. Ruhman, T. Tsuneda, M. Chiba, T. Taketsugu, T. Tahara, Science 322 (2008) 1073.

[4] Y. Suzuki, T. Fuji, T. Horio, T. Suzuki, J. Chem. Phys. 132 (2010) 174302.

[5] M. Kanno, H. Kono, Y. Fujimura, Angew. Chem. 118 (2006) 8163; Angew. Chem. Int. Ed 45 (2006) 7995.

[6] M. Kanno, K. Hoki, H. Kono, Y. Fujimura, J. Chem. Phys. 127 (2007) 204314.

[7] M. Kanno, H. Kono, Y. Fujimura, S.H. Lin, Phys. Rev. Lett. 104 (2010) 108302.

[8] M. Kanno, H. Kono, Y. Fujimura, in K. Yamanouchi et al. [Eds.], Progress in Ultrafast Intense Laser Science, VII, Springer-Verlag, Berlin, 2011, p. 53.

[9] M. Hayashi, Y. Nomura, Y. Fujimura, J. Chem. Phys. 89 (1988) 34.

[10] Y. Ohtsuki, Y. Fujimura, J. Chem. Phys. 91 (1989) 3903.

[11] From the ab initio MO results, the main vibrational modes coupled to the π-electron dynamics are the breathing mode and distortion modes of the aromatic ring, and their dimensionless potential displacements between b and c electronic states are $|\Delta cb| = 0.6$ and 0.3, respectively. Thus, the breathing mode is taken as the one-dimensional mode in the simplified model.

[12] M. Kanno, Dissertation, Tohoku University, 2009.

[13] H.-J. Werner et al., MOLPRO, version 2006.1 (Cardiff, UK, 2006).

[14] The relation can be obtained in the Condon approximation to the vibronic coupling matrix elements with a non-displaced harmonic potential for the nonadiabatic Franck–Condon vibrational overlap integral.

[15] P.M. Felker, A.H. Zewail, J. Chem. Phys. 82 (1985) 2961.

[16] H. Köppel, W. Domcke, L.S. Cederbaum, Adv. Chem. Phys. 57 (1984) 59.

[17] C. Woywod, W. Domcke, A.L. Sobolewski, H.-J. Werner, J. Chem. Phys. 100 (1994) 1400.

[18] U. Werner, R. Mitrić, T. Suzuki, V. Bonačić-Koutecký, Chem. Phys. 349 (2008) 319.